

# Improvement in the cloud mask for Terra MODIS mitigated by electronic crosstalk correction in the 6.7 $\mu\text{m}$ and 8.5 $\mu\text{m}$ channels

J. Sun<sup>1,2</sup>, S. Madhavan<sup>1,3</sup>, and M. Wang<sup>1</sup>

<sup>1</sup>NOAA National Environmental Satellite, Data, and Information Service, Center for Satellite Applications and Research, E/RA3, College Park, Maryland, USA

<sup>2</sup>Global Science and Technology, Greenbelt, Maryland, USA

<sup>3</sup>Science Systems and Applications Inc., Lanham, Maryland, USA

## ABSTRACT

MODerate resolution Imaging Spectroradiometer (MODIS), a remarkable heritage sensor in the fleet of Earth Observing System for the National Aeronautics and Space Administration (NASA) is in space orbit on two spacecrafts. They are the Terra (T) and Aqua (A) platforms which tracks the Earth in the morning and afternoon orbits. T-MODIS has continued to operate over 15 years easily surpassing the 6 year design life time on orbit. Of the several science products derived from MODIS, one of the primary derivatives is the MODIS Cloud Mask (MOD035). The cloud mask algorithm incorporates several of the MODIS channels in both reflective and thermal infrared wavelengths to identify cloud pixels from clear sky. Two of the thermal infrared channels used in detecting clouds are the 6.7  $\mu\text{m}$  and 8.5  $\mu\text{m}$ . Based on a difference threshold with the 11  $\mu\text{m}$  channel, the 6.7  $\mu\text{m}$  channel helps in identifying thick high clouds while the 8.5  $\mu\text{m}$  channel being useful for identifying thin clouds. Starting 2010, it had been observed in the cloud mask products that several pixels have been misclassified due to the change in the thermal band radiometry. The long-term radiometric changes in these thermal channels have been attributed to the electronic crosstalk contamination. In this paper, the improvement in cloud detection using the 6.7  $\mu\text{m}$  and 8.5  $\mu\text{m}$  channels are demonstrated using the electronic crosstalk correction. The electronic crosstalk phenomena analysis and characterization were developed using the regular moon observation of MODIS and reported in several works. The results presented in this paper should significantly help in improving the MOD035 product, maintaining the long term dataset from T-MODIS which is important for global change monitoring.

**Keywords:** MODIS, Terra, MOD035, Cloud detection, Electronic crosstalk, Thermal emissive bands

## 1. Introduction

MODIS, a legacy sensor, is a phenomenal work horse for the NASA's Earth Observing System, currently on board on two spacecrafts, namely the Terra (T) and Aqua (A) platforms. Since launch, T-MODIS has completed over 80,000 orbits while A-MODIS has covered over 70,000 orbits over the Earth. Together, both instruments have collected high quality geo-physical scientific data for the most part [1]. Been on orbit for this long, both MODIS instruments have their fair share of instrument related anomalies and events [2, 3]. In particular, T-MODIS has encountered higher number of significant instrument related events, the recent one being the spacecraft entering a safe mode during an inclination adjustment maneuver on February 18 2016 [4]. Since the recovery from safe mode, T-MODIS has been plagued with 21 (10 after safe mode) noisy detectors in the Long Wave InfraRed (LWIR) bands [4]. This was accompanied by large gain changes as high as 15% after the safe mode<sup>4</sup>. Prior to this, starting 2010

onwards, an increased noise level have been observed in the detector responses of the LWIR bands (i.e. bands 27-30) [2, 5-8]. This has been chiefly attributed to the electronic crosstalk contamination, which has been described with high veracity in works published in [5-16].

Clouds, an aerosol predominantly made up of tiny droplets of water and or ice are suspended all over the Earth's atmosphere. The field of climatology and other branches of Earth remote sensing has placed great importance to detection of cloud features. In order to cater to the scientific community, the MODIS atmosphere team is a dedicated house to products relating to the cloud [17-22]. Of the several cloud related products, the MODIS based cloud mask product (MOD035) is a critical output which serves it importance in the downstream processing of several Level 2 and Level 3 science retrievals. The cloud mask is a confidence flag at the pixel level marking the presence of cloud pixels at the MODIS spatial resolutions of 1 km and 250 m respectively.

In this paper, we delve into the important cloud flags based on the aforementioned LWIR bands. The paper succinctly tries to address the impact of the crosstalk contamination in T-MODIS and assess the mitigation of the correction. The improvement seen in the cloud flag is a decisive proof of the restoration for both the sensor radiometry and science based retrievals thereof. Apart from testing the improvements, the discussion section covers the possible implications for other sensors such as A-MODIS and the Suomi National Polar-orbiting Partnership (SNPP) Visible Infrared Imaging Radiometer Suite (VIIRS). The paper concludes with a synopsis of the improvements seen, providing possible directions for improved cloud detection thresholds.

## **2. MODIS Cloud Product**

The MOD035 product is a Level 2 output which classifies the presence of clouds at a pixel level. This is accomplished by employing series of threshold tests from both visible and thermal wavelengths. The product contains a 48 bit flag based on the various consistency and threshold checks [23]. Table 1, gives the partial list of the 48 bit cloud flags, in particular highlighting bits 13, 15 and 18 which are the focus for this work. The core bit flags based of thermal wavelengths comprise bits 13, 15 and 18 which will be described in some detail in the following sub-sections.

### *2.1 Bit 13*

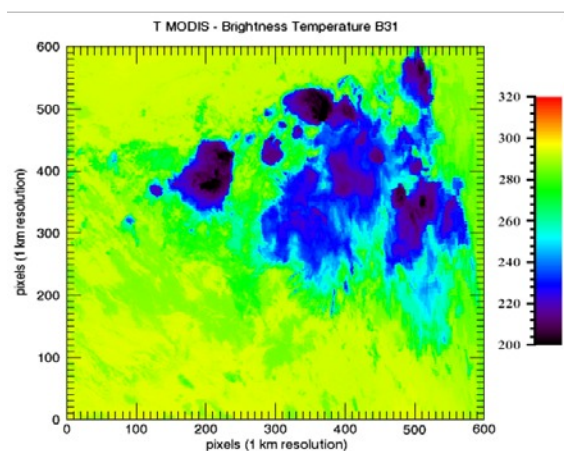
The cloud flag based of bit 13 is determined using a simple Brightness Temperature (BT) threshold from the band 31 (11  $\mu\text{m}$ ) retrieval. Such a technique works quite well when the underlying surface is mainly a water body such as ocean. The cloud features in general are much cooler in temperature (typically less than 240 K) in comparison to the ocean surface which typically ranges around 290-300 K. Thus a simple threshold value such as  $BT \leq 240 \text{ K}$  would easily suffice in positively identifying cloud pixels in the imagery. An illustration of the same is shown in Figure 1. Figure 1a depicts a cloudy T-MODIS scene from 2015105.1640 over the Pacific Ocean, the corresponding cloud mask is shown by using the above mentioned inequality threshold in Figure 1b. It is quite clear that the cloud screen based on band 31 works really well.

Table 1. Partial list of the 48 bit Cloud Mask (MOD035), highlighting the bits 13, 15, and 18 [23].

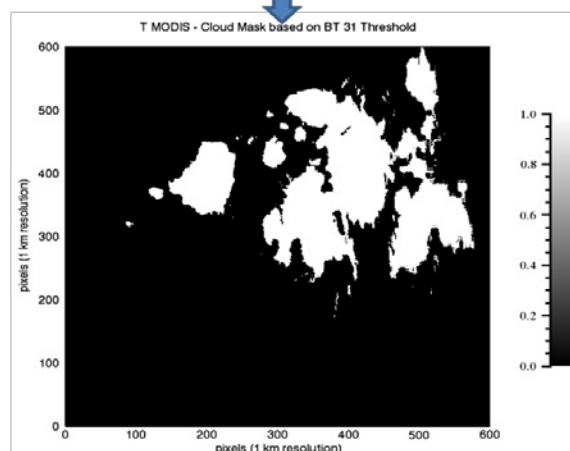
| BIT FIELD                               | DESCRIPTION KEY                                  | RESULT   |
|---|--|--|
| 0                                       | CloudMask Flag                                   | 0 = not determined<br>1 = determined   |
| 1-2                                     | Unobstructed FOV Quality Flag                    | 00 = cloudy<br>01 = probably clear<br>10 = confident clear<br>11 = high confidence clear |
| <b>PROCESSING PATH FLAGS</b>            |  |  |
| 3                                       | Day / Night Flag                                 | 0 = Night / 1 = Day  |
| 4                                       | Sun glint Flag                                   | 0 = Yes / 1 = No   |
| 5                                       | Snow / Ice Background Flag                       | 0 = Yes / 1 = No   |
| 6-7                                     | Land / Water Flag                                | 00 = Water<br>01 = Coastal<br>10 = Desert<br>11 = Land                                   |
| <b>ADDITIONAL INFORMATION</b>           |  |  |
| 8                                       | Non-cloud obstruction Flag (heavy aerosol)       | 0 = Yes / 1 = No   |
| 9                                       | Thin Cirrus Detected (solar)                     | 0 = Yes / 1 = No   |
| <b>BIT FIELD DESCRIPTION KEY RESULT</b> |  |  |
| 10                                      | Shadow Found                                     | 0 = Yes / 1 = No   |
| 11                                      | Thin Cirrus Detected (infrared)                  | 0 = Yes / 1 = No   |
| 12                                      | Spare (Cloud adjacency) (post launch)            |  |
| <b>1-km CloudFlags</b>                  |  |  |
| 13                                      | Cloud Flag - simple IR Threshold Test            | 0 = Yes / 1 = No   |
| 14                                      | High Cloud Flag - CO <sub>2</sub> Threshold Test | 0 = Yes / 1 = No   |
| 15                                      | High Cloud Flag - 6.7 $\mu$ m Test               | 0 = Yes / 1 = No   |
| 16                                      | High Cloud Flag - 1.38 $\mu$ m Test              | 0 = Yes / 1 = No   |
| 17                                      | High Cloud Flag - 3.7-12 $\mu$ m Test            | 0 = Yes / 1 = No   |
| 18                                      | Cloud Flag - IR Temperature Difference           | 0 = Yes / 1 = No   |
| 19                                      | Cloud Flag - 3.7-11 $\mu$ m Test                 | 0 = Yes / 1 = No   |
| 20                                      | Cloud Flag - Visible Reflectance Test            | 0 = Yes / 1 = No   |
| 21                                      | Cloud Flag - Visible Ratio Test                  | 0 = Yes / 1 = No   |
| 22                                      | Cloud Flag - Near IR Reflectance Ratio Test      | 0 = Yes / 1 = No   |
| 23                                      | Cloud Flag - 3.7-3.9 $\mu$ m Test                | 0 = Yes / 1 = No   |

Example: Granule id 2015105.1640

BT (Band 31)  $\leq$  240 (Cloud Mask = 1)



a.



b.

Figure 1. Demonstration of cloud flag (Bit 13) using T-MODIS granule 2015105.1640.

## 2.2 Bit 15

Bit 15 cloud flag has a unique purpose and is highly useful for discerning clear skies over Polar Regions (cold Earth view targets). The cloud detection is based on a difference threshold between Band 27 (6.7  $\mu\text{m}$ ) and Band 31 [23]. In general the surface temperatures from band 31 are much warmer than the band 27 BT responses. However, over cold targets severe surface inversion happens and the difference between band 27 and 31 can be used to identify clear pixels which otherwise would be classified as cloudy. Typical threshold limits for cloud detection are as follows:

$$\text{BT (Band 27)} - \text{BT (Band 31)} \geq -5.0 \text{ (Cloud Mask} = 1)$$

$$\text{BT (Band 27)} - \text{BT (Band 31)} \leq -5.0 \text{ (Cloud Mask} = 0)$$

## 2.3 Bit 18

The cloud flag from bit 18 is produced using the BT differences of MODIS band 29 and band 31. Band 29 corresponds to a center wavelength of approximately 8.55  $\mu\text{m}$  and plays a significant role in understanding cloud top properties. Clouds tend to be highly emissive at 8.55  $\mu\text{m}$  compared to 11  $\mu\text{m}$ . Hence a difference threshold allows detection of warm moist clouds easily. In general, clouds have a positive value in the BT differences of 8.55  $\mu\text{m}$  – 11  $\mu\text{m}$ . Thus, in order to detect the presence of clouds, the following inequality is used:

$$\text{BT (Band 29)} - \text{BT (Band 31)} > 0 \text{ (Cloud Mask} = 1)$$

$$\text{BT (Band 29)} - \text{BT (Band 31)} < 0 \text{ (Cloud Mask} = 0)$$

In the ensuing section, it will be demonstrated the impact of electronic crosstalk contamination on the cloud flags based of bit 15 and 18, followed by the dramatic improvement achieved after correcting for the same.

## 3. Testing the Improvements

The electronic crosstalk effect has been well understood and as mentioned above is copiously documented [5-16]. In the current context, the impact of the electronic crosstalk on the radiometry of band 27 and band 29 will be briefly discussed. The electronic crosstalk contamination in the LWIR bands have manifested in two ways. First, the detector responses are severely mismatched thereby causing striping noise in the imagery. Next, a long-term radiometric drift is clearly seen from typical ocean sites. Over the Pacific Ocean, the long-term drifts are in the order of - 6 K and + 1.5 K approximately for bands 27 and 29 respectively [7, 9]. With the mitigation of the electronic crosstalk correction the long-term drifts are essentially reduced to within  $\pm 0.5$  K in band 27 and within  $\pm 0.2$  K in band 29. During the course of the investigation, it has been reported there have been severe misclassifications in their cloud mask threshold tests which incorporated the aforementioned bands<sup>24</sup>. Subsequently, we tested their cloud masks based of the affected bands before and after the crosstalk correction and to our greatest satisfaction had resolved the issue. In the subsequent paragraph we document these findings and hope to delve a bit deeper in our future works.

Figures 2a and 2d shows the problem cloud masks that are based on band 27 and band 29 respectively. The dramatic improvements in the cloud masks after the electronic crosstalk correction are highlighted through figures 2b and 2e respectively. As observed, the cloud masks before the correction are significantly contaminated. In the case of the cloud mask based on band 27, there are considerable false negative classifications that are accounted for after the correction (refer Figure 2b). This is quantified using the histogram of Band 27-Band 31 BT differences for the example scene before and after the correction. After the correction, the tail of the blue curve is displaced by at least 10 K. Going by the inequality mentioned in section 2.2; the false negative classifications are removed after the shift in the BT differences of band 27 and 31. In the case of cloud mask based on band 29 and band 31 BT differences, severe false positive cloud classifications are observed (refer Figure 2d). The same is significantly alleviated after the crosstalk correction is applied. From the inequality shown in section 2.3, clouds tend to have a value greater than zero. However, as observed, significant number of pixels has a BT difference between band 29 and band 31 greater than zero (shown in red, Figure 2f). This is significantly corrected and is quantified by the negative displacement of the blue curve (i.e., after the crosstalk correction). Thus qualitatively and quantitatively, it is demonstrated that the crosstalk correction does impact the cloud mask generation, and successful mitigation of the same does improve the quality of the outputs.

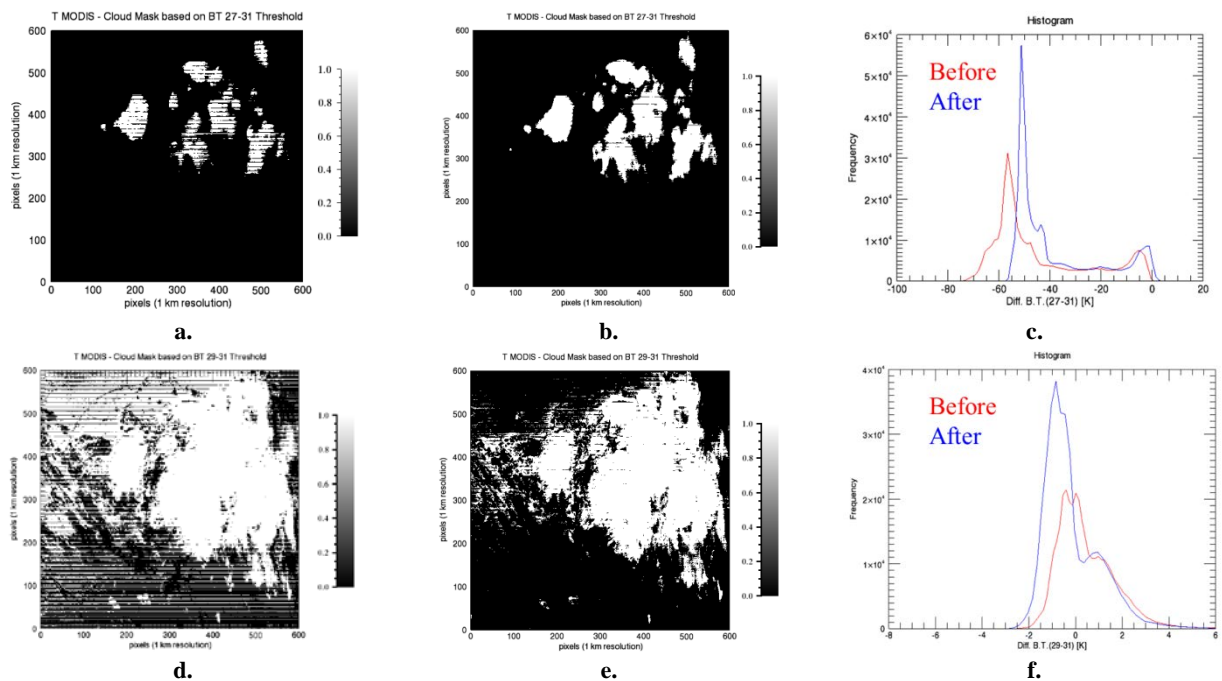


Figure 2. Improvement in cloud detection using T-MODIS, granule id. 2015105.1640. a. band 27-31 (before the correction), b. band 27-31 (after the correction), c. histogram: band 27-31 BT (before & after the correction), d. band 29-31 (before the correction), e. band 29-31 (after the correction), and f. histogram: band 29-31 BT (before & after the correction).

#### 4. Evidence for A-MODIS and SNPP VIIRS

From analyzing the moon observations from A-MODIS and SNPP-VIIRS, we reported that there is discernable crosstalk impact similar to T-MODIS however with slight differences [16]. The magnitude of crosstalk is about half or less for A-MODIS in comparison to T-MODIS. In the case of SNPP-VIIRS, the crosstalk magnitude is even smaller but non-negligible amount [16]. Given these evidences, we try to

understand the implications of the same in the cloud mask generation. In order to do so, we picked the same geographical region and the same day as T-MODIS to see the impacts. Figure 3a shows the BT differences of band 29 and band 31, with the corresponding cloud mask shown in Figure 3b. Based on these two figures, we confirm our suspicion of the electronic crosstalk through the similar false positive misclassifications as was the case in T-MODIS. Since SNPP VIIRS is built using the strong heritage of MODIS, the similar spectrally looking channels M14 and M15 are used. The BT differences of the same are shown in Figure 4a.

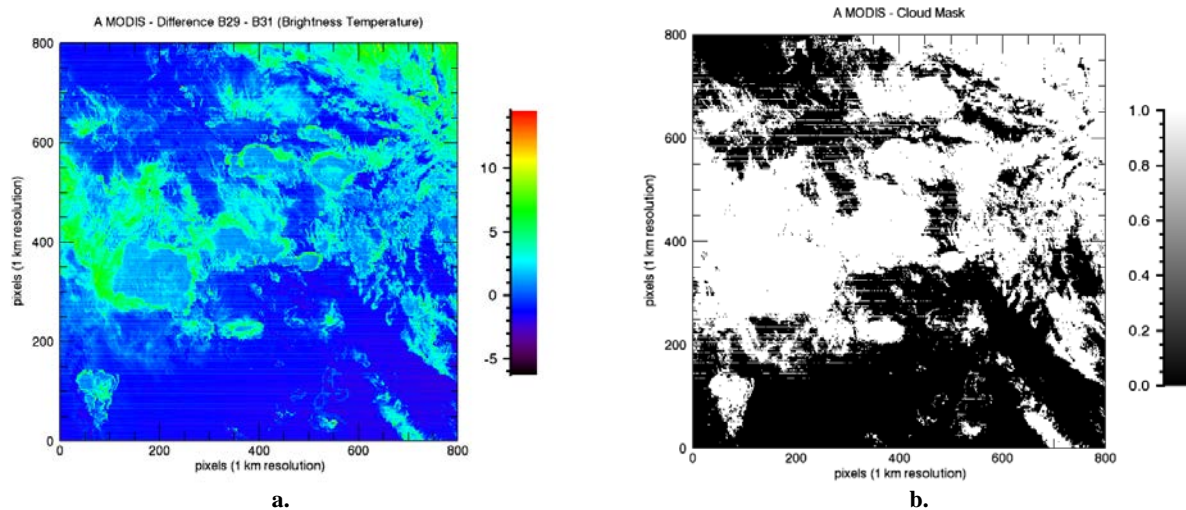


Figure 3. Cloud detection using A-MODIS, granule id. 2015105.1935. a. band 29-31 BT and b. the corresponding cloud masking.

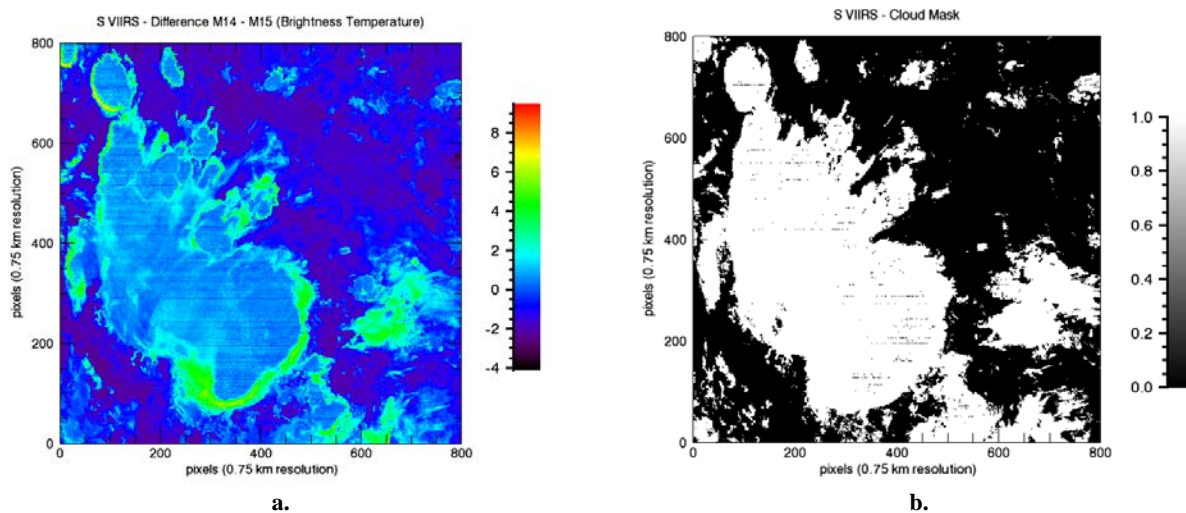


Figure 4. Cloud detection using SNPP-VIIRS, granule id. 2015105.1830. a. band M14-M15 BT and b. the corresponding cloud masking.

Figure 4b shows the resulting cloud mask based on the inequality mentioned in section 2.3. It is observed that there indeed is small amount of false negative misclassification and its probable cause to be electronic crosstalk. However, we have to conduct further characterization and mitigation to conclude that this indeed is the case. The results as seen in Figures 3 and 4 are quite eye opening that crosstalk is a



serious calibration issue and needs to be accounted for in order to maintain a sound radiometry from these affected bands.

## 5. Summary

In this paper we report the electronic crosstalk to have impacts in the cloud masks of Terra MODIS, Aqua MODIS and SNPP-VIIRS. For T-MODIS, the cloud flags (Bit 15 and 18) based on band 27 and 29 are severely affected leading to false classifications of cloud pixels, severely degrading the quality of the MOD035 cloud mask products. By mitigating the electronic crosstalk correction we demonstrated significant improvement in the corresponding cloud flag bits (Bit 15 and 18). The confidence levels of the cloud mask product should be dramatically improved after the correction. Very clear and definitive correction and improvements are demonstrated, and it is recommended this to be applied to T-MODIS. It is also demonstrated that the cloud mask products in A- MODIS and SNPP-VIIRS are also impacted by the non-negligible crosstalk effect, although may not be as severe as T-MODIS. Currently, SNPP-VIIRS band M14 performance exceeds both T- and A-MODIS (Band 29). Therefore, a strong recommendation is to use SNPP-VIIRS responses as benchmark for cloud mask thresholds.

## Acknowledgements

The authors would like to extend their thanks to Dr. Fuzhong Weng, Dr. Brij Gambhir and Dr. Mike Chu for their support. The views, opinions, and findings contained in this paper are those of the authors and should not be construed as an official NOAA or U.S. Government position, policy, or decision.

## References

1. Xiong, X., M. D. King, V. Salomonson, W. Barnes, B. N. Wenny, A. Angal, A. Wu, S. Madhavan, and D. Link, "Moderate Resolution Imaging Spectroradiometer on Terra and Aqua Missions", John Wiley & Sons, Ltd, vol. 9781118945179, pp. 53-89, 2015.
2. Madhavan, S., X. Xiong, A. Wu, B. N. Wenny, K. Chiang, N. Chen, Z. Wang, and Y. Li, "Noise Characterization and Performance of MODIS Thermal Emissive Bands", IEEE Transactions on Geoscience and Remote Sensing, vol. 54, issue 6, pp. 3221-3234, 2016.
3. Angal, A., X. Xiong, J. Sun, and X. Geng, "On-orbit noise characterization of MODIS reflective solar bands", J. Appl. Remote Sens. 0001; 9(1):094092, 2015.
4. [http://modis.gsfc.nasa.gov/sci\\_team/meetings/201606/presentations/plenary/xiong.pdf](http://modis.gsfc.nasa.gov/sci_team/meetings/201606/presentations/plenary/xiong.pdf)
5. Sun, J., X. Xiong, S. Madhavan, and B. N. Wenny, "Terra MODIS Band 27 Electronic Crosstalk Effect and Its Removal", IEEE Transactions on Geoscience and Remote Sensing, vol. 52, issue 3, pp. 1551-1561, 2014.
6. Sun, J., S. Madhavan, X. Xiong, and M. Wang, "Investigation of the Electronic Crosstalk in Terra MODIS Band 28", IEEE Transactions on Geoscience and Remote Sensing, vol. 53, issue 10, pp. 5722 - 5733, 2015.
7. Sun, J., S. Madhavan, X. Xiong, and M. Wang, "Long-term drift induced by the electronic crosstalk in Terra MODIS Band 29", Journal of Geophysical Research: Atmospheres, vol. 120, issue 9, pp. 9944-9954, 2015.

8. J. Sun, S. Madhavan, M. Wang, Investigation and Mitigation of the Crosstalk Effect in Terra MODIS Band 30. *Remote Sens.* 2016, 8(3), 249; doi:10.3390/rs8030249.
9. Sun, J., X. Xiong, Y. Li, S. Madhavan, A. Wu, and B. N. Wenny, "Evaluation of Radiometric Improvements With Electronic Crosstalk Correction for Terra MODIS Band 27", *IEEE Transactions on Geoscience and Remote Sensing*, vol. 52, issue 10, pp. 6497 - 6507, 2014.
10. Sun, J., S. Madhavan, and M. Wang (2016), Crosstalk effect mitigation in black body warm-up cool-down calibration for Terra MODIS longwave infrared photovoltaic bands, *J. Geophys. Res. Atmos.*, 121, 8311–8328, doi:10.1002/2016JD025170.
11. Sun, J., S. Madhavan, B. Wenny, and X. Xiong, "Terra MODIS band 27 electronic crosstalk: cause, impact, and mitigation", *Proceedings of SPIE – Sensors, Systems, and Next-Generation Satellites XV*, vol. 8176, no. 81760Z, 2011.
12. Madhavan, S., J. Sun, X. Xiong, B. N. Wenny, and A. Wu, "Statistical analysis of the electronic crosstalk correction in Terra MODIS Band 27 ", *Proc. SPIE 9218, Earth Observing Systems XIX*, 921824, 2014.
13. Sun, J., S. Madhavan, X. Xiong, and M. Wang, "Electronic crosstalk correction for terra long wave infrared photovoltaic bands ", *Proc. SPIE 9264, Earth Observing Missions and Sensors: Development, Implementation, and Characterization III*, 926412, 2014.
14. Madhavan, S., X. Xiong, J. Sun, K. Chiang, and A. Wu, "Electronic crosstalk characterization of Terra MODIS long wave infrared channels ", *Proc. SPIE 9607, Earth Observing Systems XX*, 96070W, 2015.
15. Sun, J., S. Madhavan, X. Xiong, and M. Wang, "Electronic crosstalk in Terra MODIS thermal emissive bands ", *Proc. SPIE 9607, Earth Observing Systems XX*, 96070V, 2015.
16. Sun, J., S. Madhavan, and M. Wang, "Crosstalk effect and its mitigation in thermal emissive bands of remote sensors", *Proc. SPIE 9972, Earth Observing Systems XXI*, current proceedings, 2016.
17. Frey, R. A. & Ackerman, S. A. & Liu, Y. & Strabala, K. I. & Zhang, H. & Key, J. R. & Wang, X. Cloud detection with MODIS. Part I: Improvements in the MODIS cloud mask for collection 5 *J. Atmos. Oceanic Tech.*, Vol. 25, pp. 1057-1072 (2008).
18. Ackerman, S. A. & Holz, R. E. & Frey, R. & Eloranta, E. W. & Maddux, B. C. & McGill, M. Cloud detection with MODIS. Part II: Validation, *J. Atmos. Oceanic Tech.*, Vol. 25, pp. 1073-1086 (2008).
19. Baum, B. A., W. P. Menzel, R. A. Frey, D. Tobin, R. E. Holz, S. A. Ackerman, A. K. Heidinger, and P. Yang MODIS Cloud-Top Property Refinements for Collection 6 *J. Appl. Meteor. Climatol.*, 51, 1145-1163 (2012).
20. Ackerman, S. A. & Strabala, K. I. & Menzel, W. P. & Frey, R. A. & Moeller, C. C. & Gumley, L. E. Discriminating clear sky from clouds with MODIS *J. Geophys. Res.*, Vol. 103, 32141-32157 (1998).
21. Yang, P., B. C. Gao, B. A. Baum, Y. X. Hu, W. J. Wiscombe, S. C. Tsay, D. M. Winker, and S. L. Nasiri Radiative properties of cirrus clouds in the infrared (8-13 $\mu$ m) spectral region *J. Quant. Spectrosc. Radiat. Transfer*, Vol. 70, pp. 473-504 (2001).
22. Liu, Y. & Key, J. R. & Frey, R. A. & Ackerman, S. A. & Menzel, W. P. Nighttime polar cloud detection with MODIS *Remote Sens. Environ.*, Vol. 92, 181-194 (2004).
23. Ackerman, Frey, Strabala, Liu, Gumley, Baum, & Menzel, "Cloud Mask Product: Discriminating Clear-Sky from Cloud with MODIS - Algorithm Theoretical Basis Document", (2010).
24. [http://modis-atmos.gsfc.nasa.gov/\\_docs/B29KnownIssueV2.pdf](http://modis-atmos.gsfc.nasa.gov/_docs/B29KnownIssueV2.pdf)